J. Membrane Biol. 156, 157–172 (1997)

The Journal of
Membrane
Biology

Influence of Cys-130 S. aureus Alpha-toxin on Planar Lipid Bilayer and Erythrocyte Membranes

O.V. Krasilnikov[1,2], **M.-F.P. Capistrano**[2], **L.N. Yuldasheva**[2,3], **R.A. Nogueira**[2]

[1]Laboratory of Molecular Physiology, Institute of Physiology and Biophysics, 700095 Tashkent, Uzbekistan
[2]Laboratory of Membrane Biophysics, Department of Biophysics and Radiobiology, Federal University of Pernambuco, 50670-901, Recife, PE, Brazil
[3]Department of biochemistry, Tashkent Pediatric Medical Institute, 700125 Tashkent, Uzbekistan

Received: 8 September 1995/Revised: 20 November 1996

Abstract. Replacement of an amino acid residue at position 130 -Gly by Cys- in the primary structure of Staphylococcus aureus alpha-toxin decreases the single-channel conductance induced by the toxin in planar lipid bilayers. Concomitantly, the pH value at which the channel becomes unable to discriminate between Cl^- and K^+ ions is also decreased. By contrast, the pH dependence of the efficiency of the mutant toxin to form ion channels in lipid bilayers was unchanged (maximum efficiency at pH 5.5–6.0). The asymmetry and nonlinearity of the current-voltage characteristics of the channel were increased by the point mutation but the diameter of the water pore induced by the mutant toxin, evaluated in lipid bilayers and in erythrocyte membranes, was found to be indistinguishable from that formed by wild-type toxin and equal to 2.4–2.6 nm.

Alterations at the ''*trans* mouth'' were found to be responsible for all observed changes of the channel properties. This mouth is situated close to the surface of the second leaflet of a bilayer lipid membrane. The data obtained allows us to propose that the region around residue 130 in fact determines the main features of the ST-channel and takes part in the formation of the *trans* entrance of the channel.

Key words: Site-directed mutagenesis — Staphylotoxin — Planar lipid bilayer — Erythrocyte — Ion channel

Introduction

The structure of Staphylococcus aureus alpha toxin (ST), and the properties of the ion channel formed by it were intensively studied during the last 20 years (Six & Harshman, 1973; Watanabe & Kato, 1978; Kato & Watanabe, 1980; Fussle et al., 1981; Gray & Kehoe, 1984; Ikigai & Nakae, 1985; Tobkes, Wallace & Bayley, 1985; Blomqvist & Thelestam, 1986; Blomqvist et al., 1987; Krasilnikov et al., 1988; Forti & Menestrina, 1989; Krasilnikov & Sabirov, 1989; Bhakdi & Tranum-Jensen, 1991; Krasilnikov, Sabirov, Ternovsky, 1991; Ward & Leonard, 1992; Olofsson et al., 1992; Hebert et al., 1992; Menestrina et al., 1992; Walker & Bayley, 1994; Jonas et al., 1994*b*). However, we are far from understanding the role of individual amino acids on the structure and function of the ion channel formed by the toxin. To address this issue two independent groups started to express mutant toxins (Palmer et al., 1993*a,b,c;* Walker et al., 1992; Walker, Krishnasastry & Bayley, 1993; Walker & Bayley; 1994). However, the properties of ion channels induced by these mutant toxins in membranes have not been investigated. Mutants were assayed in the erythrocyte test system and based on these observations the authors concluded that a small N-terminal peptide is important for the hemolytic activity of the toxin. These studies also led to the assumption that the central glycine-rich loop (the so-called ''hinge'' region) of the toxin is of little significance for oligomerization in the membrane but that it can be responsible for the ''correct structure of the conductive channel'' formed by the toxin.

Nevertheless, at least two interesting problems remain unanswered. What is the role of the glycine-rich loop in the channel structure or, in other words, what happens to the properties of the channel if the loop region is altered? Where in the tridimensional channel structure is this glycine-rich part of the toxin molecule located? To address these questions we chose to study the mutant toxin, Gly-130-Cys, where a glycine in the

Correspondence to: O.V. Krasilnikov

central region of the toxin (at position 130) was substituted by a cysteine (M-ST).

It was found that the Gly ⇒ Cys substitution at position 130 of the α-toxin of S. aureus change a number of the properties of the channel. The single-channel conductance and the pH value where the channel is unable to discriminate between Cl^- and K^+ ions was decreased. On the other hand, the asymmetry and nonlinearity of the current-voltage relationship of the channels (CVR) was increased by the substitution. However, the apparent size of the ion channel water lumen and the channel-forming ability of the toxin were basically not altered. Use of a direct method to establish the localization of Cys130 in the channel structure with specific SH-reagents was not successful. However, using asymmetrical planar bilayer lipid membranes (PLM) and distinctly oriented salt gradients and pH shifts allowed us to obtain convincing evidence that all observed alterations of the channel properties are mainly determined by changes in the *trans* entrance of the channel (we define the *cis* side as the side where the toxin is added). The data strongly suggest that the *trans* entrance is situated close to the surface of the second leaflet of the lipid membrane and that the region around residue 130 takes part in the formation of the *trans* entrance of the ST-channel.

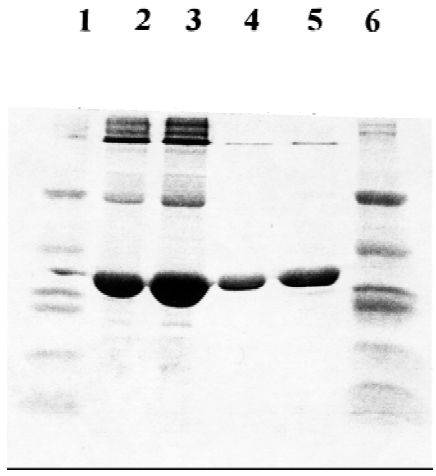

Fig. 1. Sodium dodecyl-sulfate polyacrylamide gel electrophoresis of wild and M-ST. Lanes 2 and 4; wild-type ST, 15 μg and 3 μg of protein was loaded in each lane respectively; lanes 3 and 5; M-ST, 17 μg and 3.5 μg was loaded in each lane respectively. The samples were not boiled in presence of SDS in order to observe all (covalent and non-covalent) aggregates. When samples were boiled (5 min 95°C) in the presence of SDS the amount of aggregated forms was decreased and practically all the protein was visualized as a single band at 34 kDa-zone (*data not shown*). Preliminary heating of M-ST-sample at 50°C for 20 min lead to aggregate formation (dimer, tetramer and larger). Some of the aggregates could be dissociated by boiling (5 min 95°C) in the presence of SDS and all of them were dissociated when the boiling was done in the presence of SDS and dithiotreitol or β-mercaptoethanol (*data not shown*). Marker proteins were purchased from Sigma (lanes 1 and 6): β-galactosidase—116 kDa; phosphorylase b—97.4 kDa; bovine serum albumin—66 kDa; egg ovalbumin—45 kDa; bovine carbonic anhydrase—29 kDa; soybean trypsin inhibitor—20.1 kDa; lysozyme—14.3 kDa.

Materials and Methods

Chemicals

Pure phosphatidylcholine was prepared according to Bergelson et al. (1981) or purchased from Sigma (Type V-E). Azolectin (Type II, Sigma) was purified by acetone extraction (Kagawa & Racker, 1971). Cholesterol, N-methylmaleimide (NMM), 5,5′-dithio-bis-(2-nitrobenzoic acid) (DTNB), iodacetamide (IAA), phenylmethylsulfonyl fluoride (PMFS) and dithiothreitol (DTT) were purchased from Sigma and used as received.

The wild-type (ST) and mutated alpha-toxin (Gly-130-Cys), designated M-ST, were donated by Prof. S. Bhakdi and Dr. M. Palmer (Institute of Medical Microbiology, University of Mainz, Germany). Homogeneity of the toxins used was confirmed by sodium dodecyl-sulphate-polyacrilamide gel electrophoresis (SDS-PAGE). Figure 1 shows that most of the toxin is in a monomeric form. A small percentage of oligomers and negligible amounts of fragments are also recognizable. To ascertain the correct properties of the M-ST sample used by us some of its known features: formation of dimers in the solution after heating to 50°C and its dissociation by DTT were examined and found to be analogous to those described by Palmer and coauthors (Palmer et al., 1993*b*) for this mutant toxin.

Most of the data on the properties of ion channels induced by the ''N-terminal fragment'' of wild ST (F-ST) was taken from Krasilnikov et al. (1991) and Ternovsky et al. (1991). In short, the methods of trypsin treatment and F-ST purification were as follows: Wild-type ST was solubilized in 10 mM Tris, pH 7.2 at a concentration of approximately 2 mg/ml. Then trypsin (Boehring, Germany) was added (40 μg/ml) and the mixture was kept for 4 h at 37°C. Proteolysis was stopped by addition of 1 mM PMFS or directly submitting the sample to preparative isoelectric focusing. SDS-PAGE electrophoresis demonstrates that the trypsinized toxin does not contain visible amounts of the whole molecule. Most of the trypsin-treated material ran as 14–18 kDa band. This set of proteolytic products practically loses all hemolytic activity. That is due, obviously, to the removal of the small NH_2-terminal peptide through cleavage after Lys-8 (Walker et al., 1993). Strikingly the proteolytic products still demonstrate a strong channel-forming activity in planar lipid bilayer membrane experiments (about 10% of that observed for the whole toxin). The proteolytic products (after weak trypsin digestion) were separated by preparative isoelectric focusing. A minor protein band (corresponding to about 5% of the total peptides in the mixture) with isoelectric point ~8.2 was taken and as shown by Ternovsky et al. (1991) in SDS-PAGE, it ran as a single peptide band with molecular mass close to 16 kDa. In principle, based on data of Palmer et al. (1993*c*) one can tell that this peptide may be really a nicked version of the whole toxin.

Proteinase K treated ST (K-ST) was obtained with the method described by Palmer and coauthors (Palmer et al., 1993*c*). K-ST retained about half of the hemolytic activity of the whole toxin and basically the same level of channel-forming activity of wild ST (*unpublished data*).

Ethylene glycol, glycerin and glucose were bought from Merck; sucrose was purchased from Reagen. We used poly(ethylene glycol) (PEG) with an average molecular mass (Da): 200, 300 and 400 (Sigma); 600 (Riedel de Haën); 1000, 1500, 2000, 3000, 4000, 6000 (Loba Chemie). All nonelectrolyte polymers were additionally purified by anion-exchange chromatography by using the strong alkaline

anion exchangers III or IV (Merck). This treatment removed anion-group contained contaminations that decrease PLM stability (life time) and increase probability of the ion channel transitions from open to closed states. Hydrodynamic radii of nonelectrolytes were taken from Krasilnikov et al. (1991, 1992) and Sabirov et al. (1993). Other chemicals were analytical grade and used without additional purification.

Water double distilled in glass was used in the preparation of all buffer solutions. For bilayer experiments, two basic solutions were used. The first contained 0.1 M KCl, 0.005 M. Tris-OH, and the pH was adjusted to the appropriate value by citric acid—(buffer 1). Sometimes this buffer contained DTT at a final concentration of 1–10 mM. The second buffer contained 0.1 M KCl, 0.005 M KH_2PO_4. The pH was adjusted by 1.0 M KOH (buffer 2). For erythrocyte experiments, the basic solution contained 0.15 M NaCl, 0.005 M Tris-OH, and the pH was adjusted by 1.0 M HCl to pH 7.5 (buffer 3).

Planar lipid bilayer membranes (PLM) were formed at room temperature (25 ± 2°C) by the technique of Montal & Mueller (1972). When noted, bilayer was formed by Mueller method ((BLM) Mueller et al., 1963) and give the same results. A 1–2% lipid solution in *n*-decane was used to form bilayers by the Mueller method. A binocular microscope was used to control the BLM formation. When we used the Montal & Mueller technique, monolayers from a 10 mg/ml solution of the lipids in *n*-hexane were spread on the surface of two buffered salt solutions (4 ml) separated by a 25 μm thick Teflon partition in a Teflon experimental cell. After evaporation of the solvent, the membrane was formed by raising the monolayers above the level of the hole (~0.1 mm in diameter) which had been pretreated with a 2% solution of Vaseline in *n*-hexane. During the bilayer formation, the peak current in response to a square wave (amplitude, ±5–10 mV; frequency, ~500 Hz) was monitored continuously.

Experiments were done under voltage-clamp conditions. The current that was going through the bilayers was measured with Ag/AgCl electrodes connected through salt bridges (3% agar with 3 M KCl) in series with a voltage source and a current amplifier (K284UD1A). The *trans* compartment of the experimental chamber was connected to the virtual ground. Voltage pulses were applied to the *cis* compartment of the chamber. The amplifier signal was monitored with a storage oscilloscope and recorded on a strip chart or tape recorder.

After the membrane was completely formed and stabilized, a few μl of the stock solution containing a channel-forming protein (1 mg/ml) was added to one compartment of the experimental cell with concentrations ranging from 0.2 μg/ml to 4 μg/ml (for multichannels experiments). The solutions in both compartments were magnetically stirred. When conductance of the bilayers reached approximately 10 nS, the toxin-containing solution was replaced by a fresh buffer. The increase in bilayer conductance stopped within a few minutes. These bilayers were then used for measuring instantaneous current voltage characteristics, selectivity and the effects of SH-specific reagents.

The conductance of the bilayer membranes (G) in symmetrical solutions was defined as $G = I/V$, where I is the transmembrane current flowing through the channels and V corresponds to the fixed potential. Basal conductance of PLM was less than 4 pS for PC bilayers and approximately 5 pS for azolectin bilayers.

The selectivity of the ion channels was measured in the presence of a threefold KCl concentration gradient (300 mM/100 mM KCl or 100 mM/300 mM KCl, *cis*/*trans*). Zero current potential was defined as the potential (V^*) that must be applied to the experimental cell to reach a virtual zero transmembrane current equal to that of a symmetrical system with zero mV applied potential.

To record the instant current-voltage relationship (CVR), the transmembrane potential was initially increased stepwise from zero to minus 140–150 mV and then gradually increased to 140–150 mV (during a voltage ramp with duration of 200–250 msec). Finally, the transmembrane potential was returned stepwise to zero mV (''minus ⇒ plus'' experiment). The reversal of the voltage protocol (''plus ⇒ minus'' experiments) gave the same type of CVR. To decrease current noise the stirring was sometimes stopped when we measured the CVRs. The relationship between the current going through the channels incorporated in BLM at −100 mV and its value at +100 mV (I_{-100}/I_{+100}) was taken as a quantitative measure of CVC asymmetry (A) (the sign referred to the side of the protein addition). To evaluate nonlinearity (L) we used a relation between values of the membrane conductance at ±100 mV and ±20 mV (G_{100}/G_{20}).

N-methylmaleimide (NMM), 5,5′-dithio-bis-(2-nitrobenzoic acid) (DTNB) and iodacetamide (IAA) were applied to bilayers doped with M-ST at final concentrations of 1.0 mg/ml, 0.06 mg/ml and 1.0 mg/ml, respectively. In these experiments, standard buffer 2 was used. Stock solutions of the chemicals were prepared just before experiments: N-methylmaleimide (NMM)—100 mg per ml of dimethylsulfoxide; 5,5′-dithio-bis-(2-nitrobenzoic acid) (DTNB)—50 mg per ml water, and the pH was adjusted by KOH to 7.0; iodacetamide (IAA)—100 mg per ml of water. The pH value in the compartments of the experimental cell was verified after each experiment.

Channel-sizing Experiments

The maximal size of the channel incorporated in planar lipid bilayer membranes was tested by the recently described method of Krasilnikov et al. (1992). In short, nonelectrolyte molecules with different hydrodynamic size were used as molecular probes. Usually the single-channel conductance was examined in the presence of 20% of one of the nonelectrolytes in buffer 1 (pH 7.5). Mean values of the single-channel conductances and the solution conductivities were used to establish a permeability parameter, V, which was calculated as:

$$v = (G_o - G)/G_o : (H_o - H)/H_o$$

Where H_o and G_o are the electrical conductivity of 0.1 M KCl and the channel conductance in this same solution, respectively; H and G are the electrical conductivity of 0.1 M KCl solution containing 20% nonelectrolyte and the channel conductance in this same solution, respectively.

The maximal radius of the water pore of the channels was taken equal to the minimal hydrodynamic radius of an impermeable nonelectrolyte molecule, i.e., a molecule which does not decrease an ion channel conductance at all. In practice it was determined from the dependence of parameter v on the hydrodynamic radius of nonelectrolytes. It was determined as the point of transition from the linear falling part to the lower horizontal branch of the permeability parameter dependence on the hydrodynamic radius of nonelectrolytes.

The osmotic balance method was used by us to measure the radius of water pores induced by ST and M-ST in erythrocyte membranes. The nonelectrolytes were previously added into standard buffer-3 with a final concentration (mM): ethylene glycol (80), glycerol (80), glucose (80), sucrose (80), poly (ethylene glycol) (PEG) 400 (80), PEG 600 (72), PEG 1000 (65), PEG 1500 (55), PEG 2000 (46), PEG 3000 (40), PEG 4000 (31), PEG 6000 (24). The increase in solution osmolarity after the addition of each nonelectrolyte was identical and equal to 80 milliOsmoles per liter as measured by freezing point depression with an OMKA 1C-05 osmometer. This osmolarity value was about two times greater than that found for hemoglobin in erythrocytes (Adair, 1929; and our *unpublished data*).

Rabbit erythrocytes were prepared from fresh blood that was stabilized by EDTA. After being washed three to four times by standard buffer-3, the erythrocyte concentration was adjusted to 4% (v/v). A volume of solution containing ST (or M-ST) was diluted with the desired nonelectrolyte solution and placed into plastic tubes that were

vigorously mixed with an equal volume of 4% suspension of rabbit erythrocytes (in standard buffer 3). The final concentration of erythrocytes was 2%. The final increment of solution osmolarity created by the nonelectrolytes was practically equal to that generated by intracellular hemoglobin. We hoped that by using a fixed 40 mOsm/liter-increment (with varying nonelectrolyte concentrations) we would get a better data set than those previously published that were obtained at constant concentrations of nonelectrolytes (Fussle et al., 1981; Bhakdi, Muhly & Fussle, 1984; Katsu et al., 1988; Thelestam & Blomqvist, 1988; Krasilnikov et al., 1988; Sabirov, Zakhidova & Krasilnikov, 1991).

The extent of lysis was estimated in appropriate time intervals by two methods. The first was based on determining the optical density (OD) of the supernatant (after centrifugation of an aliquot of the erythrocyte suspension) at 540 nm. In the second method, the extent of lysis was quantified by direct measurement of the cell suspension's OD (at 710 nm). At this wavelength the lysis caused a decrease of the OD value. To quantify the extent of hemolysis, an aliquot (100–150 μl) of cell suspension was added to 4 ml of standard buffer-3 containing the appropriate type of nonelectrolyte (40 mOsm), then it was vigorously mixed and the absorbance was determined at 710 nm. This method eliminates a centrifugation step in the process. The linearity of the hemolysis scale was verified by determining the differences between the optical density of serially diluted suspensions of intact cells and after these cells were lysed by triton X-100. Within the time range where it was possible to apply both methods the results obtained were essentially the same. The percentage of hemolysis calculated with erythrocytes lysed by distilled water or by 1% Triton X-100 was taken as 100%. The experiments were done at 37 ± 1°C. The apparent radius of toxin-induced water pores in erythrocyte membranes was determined to be equal to the minimal hydrodynamic radius of nonelectrolyte molecules which completely protected red blood cells against the toxin action. The Renkin plot (Renkin, 1954; Ginsburg & Stein, 1987) was also used to evaluate the apparent size of the toxin induced pores.

Protein concentration was determined with a Bradford reagent (Bio-Rad) using bovine serum albumin as the standard. Sodium dodecyl-sulfate polyacrylamide gel electrophoresis was performed according to Laemmli (1970).

The conductivity of each buffer solution was measured with conductivity meter HI 9033 (Hanna Instrument).

Results and Discussion

Ward et al. (1994) using Förster dipole-dipole energy-transfer measurements demonstrated that when M-ST was reconstructed in liposomes Cys130 was situated close to the inner leaflet of the liposome membrane. We expected to find similarities between channels formed by wild-type and mutated ST based on observations that the mutant is able to form heptamerical aggregates on the surface of erythrocytes as well as to lyse these cells in a way similar to the wild-type toxin (Palmer et al., 1993*a*,*b*).

In planar lipid bilayer experiments one would expect to establish, rather easily, the localization of the Cys-containing loop of the toxin in the tridimensional channel structure in bilayers doped with the M-ST, direct application of SH-specific reagents to either side of the experimental chamber should promote changes of the channel features, suggesting the localization of Cys

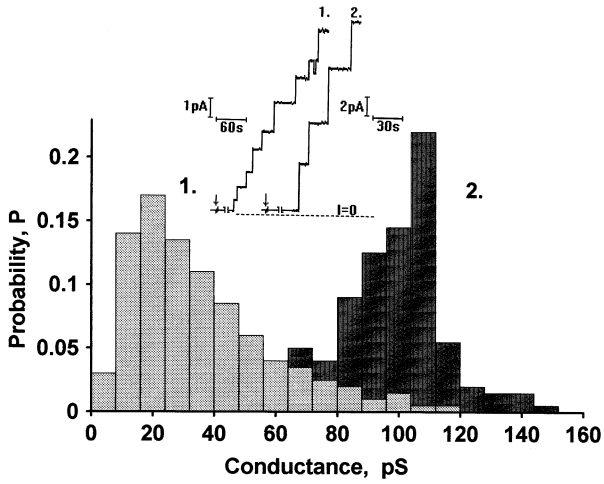

Fig. 2. The amplitude histogram of conductance fluctuations induced by M-ST **(1)** and by wild toxin **(2)** at voltage-clamped (−50 mV) phosphatidylcholine-cholesterol (1:1, by mass) membranes formed by the Mueller-method in 0.1 M KCl, 0.005 M Tris-citrate, pH 7.5. The probability, *P*, of observing steps in channel conductance like those in the current traces is represented. Bin width 8 pS. More than 800 and 200 events were observed (5–7 channels for membrane) for M-ST and for wild toxin respectively. The record was stopped if any of the open channels temporarily closed. Proteins were added in the *cis*-compartment. The original single-channel recordings are inserted. The dashed line indicates a zero current, while arrows indicate additions of the toxin (1–2 nM). Conductance and time scales are given in the figure. In separate experiments dithiothreitol (DTT) was added to the bathing solution (1–10 mM final concentrations) before the addition of M-ST and it did not change conductance or other properties of the M-ST channels.

130. However, the first records with the M-ST induced channels in PLM already demonstrated considerable difference in the conductances of the channels induced ST and M-ST. This finding was a first indication of changes in the channel structure induced by the substitution. This precluded the studies on the localization of the Cys in the channel structure and force us to, initially, make a complete characterization of the properties of the M-ST-formed ion channel.

M-ST Forms Ion Channels in Lipid Bilayers

As expected, it was found that the addition of M-ST to the voltage-clamped lipid bilayer led to a stepwise increase in the membrane conductance (Fig. 2). This indicates the formation of ion channels in the membrane. The mean channel conductance was around 20 pS and rare events exceeded 50 pS. This single-channel conductance is much smaller than that recorded for the wild toxin (80–120 pS, Fig. 2; *see also* Krasilnikov, Ternovsky & Tashmukhamedov, 1981; Krasilnikov et al., 1988; Menestrina, 1986). The presence of 1 mM DTT did not change the distribution of single-channel conduc-

tances. The presence of 1 mM DTT did not change the distribution of single-channel conductances. This suggests that under our experimental conditions disulfide bridges are not formed, and M-ST molecules in solution are therefore monomeric. The relatively low conductance of the mutated oligomeric pore (channel) in PLM reflects a real difference between the structures of wild-type and mutated channels.

In general, the difference in conductances between the ion channels induced by M-ST and by wild ST may be determined by at least two causes: (i) by difference of charges distributed near the ion channels' mouth and/or (ii) by difference in the water pore size. To examine the contribution of the first of these possibilities we determined cation/anion selectivity and current-voltage relationship (CVR) of the channels. The water pore size of the ion channel was tested in PLM- as well as in rabbit erythrocyte experiments.

The Cation-Anion Selectivity of M-ST Modified PLM

It is well known that cation/anion selectivity and current-voltage relationship (CVR) of the channels are dependent upon pH. Hence to make a fair decision about charge distribution around the ion channels' mouth it is necessary to analyze the pH-dependencies of its cation-anion selectivity as well as the CVR.

The selectivity of the two types of ion channels was evaluated measuring the zero current potential in the presence of a threefold KCl concentration gradient (300 mM/100 mM KCl, *cis*/*trans*). It was established (Fig. 3*A*) that at pH <5.7 the ion channels formed by M-ST in phosphatidylcholine (PC) bilayers were more permeable to chloride than to potassium ions. At pH ≈ 5.7 the channels were not able to discriminate between Cl and K ions. This pH (5.7) is much lower than the equivalent pH for lack of selectivity in bilayers containing channels formed by the wild toxin (pH ≈ 10; Fig. 3*A;* see also Krasilnikov et al., 1991).

As it was shown recently (Krasilnikov et al., 1989; 1991), the cation-anion selectivity of *large* water-filled channels (pores) (as ST-channel for example) is well described by the sum of electrical potentials at both channel entrances. At the same time, the current-voltage relationship (CVR) is sharply dependent on the actual values of the potential at each entrance of the channel. At each entrance, the effective potential is a superposition of electrical potentials generated by all ionogenic (titratable) groups that are in the proximity of the channel entrances. The contribution of the each group is dependent on the distance between this group and the central region of the channel entrance. Taking the above argument into account and the measured values of cation-anion selectivity of M-ST and ST channels we can conclude that *the distribution of titratable charges around the ion channel mouths is altered* by the Gly ⇒ Cys substitution at position 130 of the toxin. Moreover, we can assume that *ionogenic* (*titratable*) *groups which are able to generate negative potentials play a larger role in determining the selectivity of M-ST channels than in wild type ST channels.*

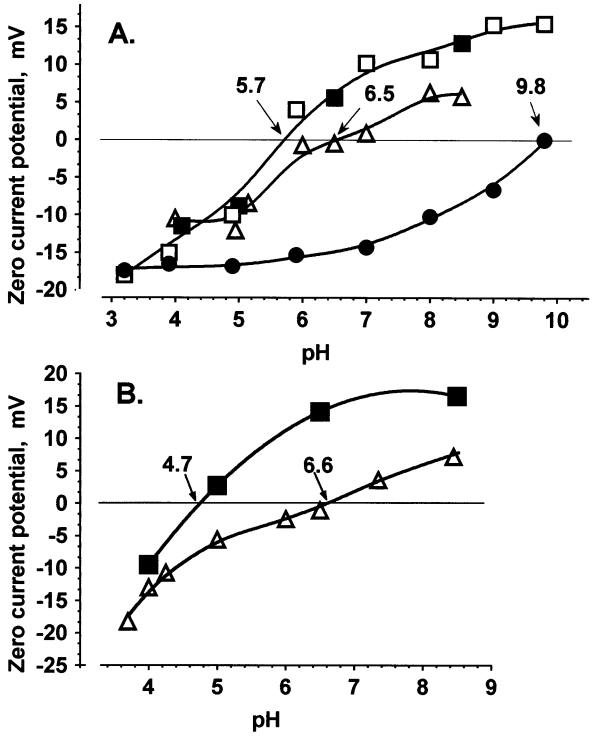

Fig. 3. Effects of pH on the zero current potential of doped bilayers formed from phosphatidylcholine (*A*) and azolectin (*B*). (*A*) PLM was formed from phosphatidylcholine-cholesterol mixture (3:1; by mass). (*B*) PLM was formed from azolectin-cholesterol mixture (3:1; by mass). The Montal & Mueller technique and the Mueller method were used with the same results. The toxin was added to the *cis* compartment of the experimental chamber at a final concentration of 0.5–2.5 μg/ml. ■—300 mM/100 mM (*cis*/*trans*) KCl system, M-ST; △—100 mM/300 mM (*cis*/*trans*) KCl system, M-ST; ● and □ - 300 mM/100 mM (*cis*/*trans*) KCl systems for PLM modified by wild toxin and by F-ST, respectively (data taken from Krasilnikov et al., 1988, 1991; and Ternovsky et al., 1991). The signs of the values of zero current potentials obtained for 300 mM/100 mM (*cis*/*trans*) KCl system are inverted to allow a better comparison of the curves. All KCl solutions were buffered by 5 mM citrate-Tris. Each value presented is the mean of 3–7 separate experiments. Other experimental conditions are given in Materials and Methods and in the text.

The Current-Voltage Relationships (CVR) of Membranes Modified by M-ST

To check the depth and localization of structural changes in M-ST channels we investigated its CVR in PC-membranes comparing it to CVR obtained from these

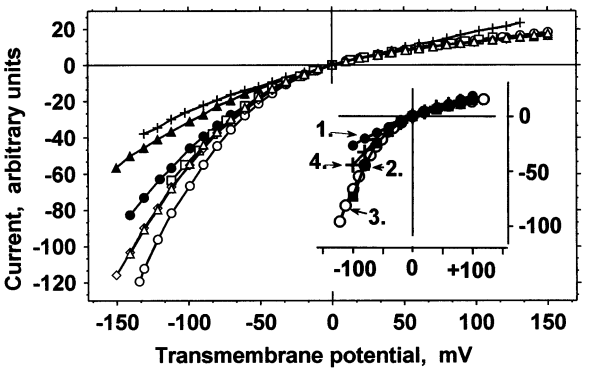

Fig. 4. Current-voltage relationships of bilayers modified by M ST. PLM was formed from a phosphatidylcholine-cholesterol mixture (3:1; by mass). The Montal & Mueller technique was used. If not mentioned, buffer 1 with indicated pHs was used. In separate experiments the concentration of KCl was increased to 3.0 M. M–ST (0.01–2.5 μg/ml; depend on pH value) was added to the *cis*-side of PLM. After the PLM conductance reached a quasi steady-state value, the CVR was measured. A voltage pulse was applied to the *cis* compartment. Protocol of voltage change is described in Materials and Methods. Results of separate experiments are presented. Symbols at 100 mM KCl: □—pH 9.0; △—pH 8.0; ○—pH 7.0; ◇—pH 6.0; ●—pH 5.0; ▲—pH 4.0; and + −3.0 M KCl, pH 8.0. Insert: Current-voltage relationships of PC-bilayers modified by wild (ST (1), F-ST (2.; data taken from Krasilnikov et al., 1991; and Ternovsky et al., 1991) and M-ST (3.); 4.—CVR of asymmetrical PLM (PC/AZ: *cis*/*trans*) modified by wild ST. In all cases, 100 mM KCl solution with pH 7.5 was used. Current scale is in arbitrary units. CVRs were normalized at 20 mV.

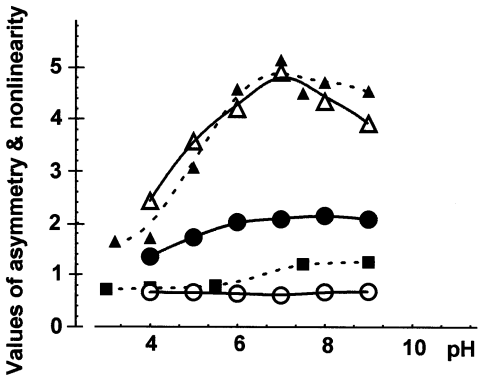

Fig. 5. The pH-dependencies of asymmetry and nonlinearity of CVR in bilayers modified by M-ST, wild ST and F-ST. Symbols: ○, ● and △—nonlinearity at positive and negative potentials; and asymmetry for PLM modified by M-ST, respectively. Symbols: ▲ and ■—asymmetry for BLM modified by F-ST (data taken from Krasilnikov et al., 1991; and Ternovsky et al., 1991) and wild ST, respectively. Each presented value is the result of 4–10 separate experiments. Buffer 1 was used. Other experimental conditions are the same as in the legend to figure 4 and in the text. Analogous results were observed with azolectin PLM (*data not shown*).

same membranes modified by wild toxin. We found that the CVR of the M-ST channels was drastically different from that of wild ST channels. CVR of the M-ST channels exhibits sharp nonlinearity (*L*) and asymmetry (*A*) (Fig. 4) The increase in electrolyte concentration in the bathing solution transformed the CVR to the more symmetrical and linear shape (+ curve in Fig. 4). Consequently, the energetic barrier(s) for passing ions (that exists in M-ST-formed ion channel water lumen and provides the shape of CVR) is mainly determined by the charges.

The amplitude of changes in parameters *A* and *L* of M-ST channels with pH is strongly different from the analogous changes in the parameters of the ion channel induced by wild ST. So *A* was relatively small at pH 4.0 (2.4 ± 0.14), increasing with pH to a maximum of 4.9 ± 0.5 at pH 7.0, and then slightly decreasing with further increases in pH (Fig. 5). The comparison of these results with data obtained with bilayers modified by wild toxin (Fig. 5; 0.9 ± 0.1 and 1.5 ± 0.2, at pH 4.0 and pH 7.0, respectively; Krasilnikov & Sabirov, 1989) points out that *ionogenic* (*titratable*) groups are much more asymmetrically distributed between the two entrances of the channel formed by the mutant toxin than by the wild type one.

In the experiments described above we showed that the properties of the ST-induced ion channel were changed considerably by the Gly → Cys substitution at position 130. We wondered if the diameter of the ion channel water pore was also changed.

To measure the size of M-ST-induced ion channel in PLM we have used the method described in detail earlier (Krasilnikov et al., 1992). It was developed for water-filled pores and has been successfully applied to determine the sizes of different ion channels including the channels induced by wild-type ST (Krasilnikov et al., 1988, 1991). To examine the radius of water pores induced by M-ST in PLM, we investigated the changes of both the solution conductivity and the mean channel conductance resulting from the addition of different nonelectrolytes to the aqueous solution bathing the bilayer. For analysis of the changes of these values and the determination of the pore size of the ion channels we had to use a permeability parameter, *v*, which was calculated as described in Material and Methods.

Determining the permeability parameter for each nonelectrolyte we found that the parameter depends on the effective hydrodynamic radius of nonelectrolyte molecules (Fig. 6). The numerical values of the parameter *v* were close to one for nonelectrolytes with small hydrodynamic radii. Therefore, the channels are well permeable to the molecules of these nonelectrolytes. The value of parameter *v* decreased from one to zero when the size of nonelectrolyte molecules increased. This implies that the concentration of the nonelectrolyte molecules in the lumen of the ion channels was smaller than in the bulk solution. Finally, the values of parameter *v* for impermeant large nonelectrolytes (PEG 2000, 4000 and 6000) reached the lowest steady-state value. In this case, pa-

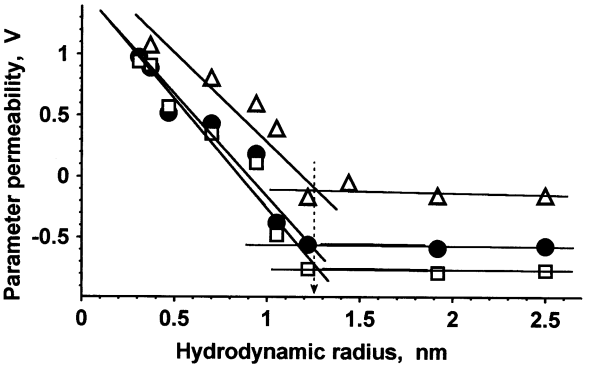

Fig. 6. Dependence of the parameter *v* on hydrodynamic radius of nonelectrolyte. Symbols: ●—M-ST channels; □—F-ST channels (taken from Krasilnikov et al., 1991); △—wild ST channels (taken from Krasilnikov et al., 1988). The permeability parameter *v* of each nonelectrolyte was calculated as described in the text. Buffer 1 (with pH 7.5) and buffer 1 containing 20% of the appropriate nonelectrolyte were used. The hydrodynamic radii of nonelectrolytes, which were taken from Krasilnikov et al. (1991, 1992) were the following: 0.26 ± 0.02 nm ethylene glycol, 0.31 ± 0.02 nm glycerin, 0.37 ± 0.02 nm glucose, 0.6 ± 0.03 nm poly(ethylene glycol) (PEG) 300, 0.7 ± 0.03 nm PEG 400, 0.94 ± 0.04 nm PEG 1000, 1.05 ± 0.04 nm PEG 1500, 1.22 ± 0.04 nm PEG 2000, 1.92 ± 0.03 nm PEG 4000, and 2.5 ± 0.03 nm PEG 6000. More than 200 ion channels were registered (5–7 channels per membrane) for each experimental condition. Arrow indicates maximal values of the radius of induced water pores established by the method. All other experimental conditions are as described in the legend to Fig. 2 and in the text and in Materials and Methods.

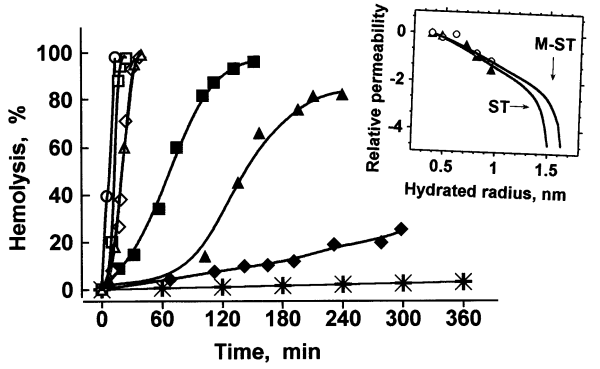

Fig. 7. Influence of nonelectrolytes on hemolytic activity of M-ST. Temperature = 37 ± 1°C. Buffer 3, pH 7.5. The results of a typical experiment are represented. Symbols: ○—control (buffer 3); □—glucose; ◇—sucrose; △—PEG 300; ■—PEG-600; ▲—PEG 1000; ♦—PEG 1450; *—PEG 2000, PEG 3000 and PEG 4000. Others experimental conditions are described in Material and Methods and in the legend of Fig. 6. Insert. Renkin plot reporting the relative diffusion rate of the osmoprotectant molecule (as compared to glucose) *vs.* its size. Relative permeability is presented in Log-scale. Hydrodynamic radius is presented in nm. Symbols: ▲—ST-pore; ○—M-ST pore. Solid lines are a best fit according to the Renkin equation (Renkin, 1954; Ginsburg & Stein, 1987), yielding functional radii of the induced pores of 1.66 ± 0.03 nm and 1.52 ± 0.03 nm for M-ST and ST induced pores, respectively.

rameter *v* had a slightly negative value because the mean ion channel conductance (*G*) in the presence of these nonelectrolytes in the buffer solution was larger than the conductance without any nonelectrolyte (G_o). At the same time the conductivity of any nonelectrolyte containing solution remained smaller than the conductivity of nonelectrolyte free solution.

Using this method we assumed that the maximal radius of water pores of M-ST-induced ion channels is determined by the intersection of the linear falling part and the horizontal branch of the permeability parameter dependence on the hydrodynamic radius of nonelectrolytes (Fig. 6). The error of the pore radius estimation was based on the standard deviation of nonelectrolytes' radii and on accuracy of determination of mean ion channel conductance. In this way we established that *the maximal radius of the ionic channel water pore formed by M-ST in planar bilayer is in the range of 1.2 to 1.3 nm* (*Fig. 6*). *The size of water pores formed by wild ST in PLM was the same* (*Fig. 6*).

To examine the apparent size of M-ST formed pores in erythrocyte membranes the osmotic balance method was used. High hemolytic activity of M-ST (comparable to that of the wild toxin) was recently demonstrated (Palmer et al., 1993*b;* Ward et al., 1994). We established that large uncharged macromolecules (PEG 3000, for example) added to the extracellular medium completely protected rabbit erythrocytes from lytic action of M-ST. This result indicated that the hydrodynamic diameter of hemoglobin molecules is larger than the size of the toxin-induced pores. The effect of PEG 3000 was not due to interference between the nonelectrolyte and toxin molecules binding to erythrocyte membranes since a simple dilution of the whole suspension by fresh buffer (buffer 3) led to fast irreversible hemolysis. The data indicate that M-ST induced hemolysis occurs by an osmotic mechanism similar to the mechanism of action of the wild toxin.

The inhibitory effect of nonelectrolytes depended on the hydrodynamic radius of their molecules. We found that macromolecules of nonelectrolytes, such as PEG 2000, PEG 3000 and other PEGs with a higher molecular mass completely inhibited the M-ST-induced lysis of rabbit erythrocytes. The result was the same if the incubation was prolonged to 8 hr and the toxin concentration was raised to 100 nM (~3.3 μg/ml) (Fig. 7). The smaller nonelectrolytes, such as glucose, sucrose, PEG 300, PEG 600, PEG 1000 and even PEG 1500 did not avoid hemolysis. The minimal hydrodynamic radius of nonelectrolyte molecules (PEG 2000) which completely prevented the M-ST-induced cell lysis was close to 1.22 nm. Considering that the accuracy of this simple semiquantitative method does not exceed 0.1 nm we can conclude that *the apparent radius of water pore induced by M-ST in the membranes of target cells is equal to 1.22 ± 0.1 nm. The same size was determined by us in parallel*

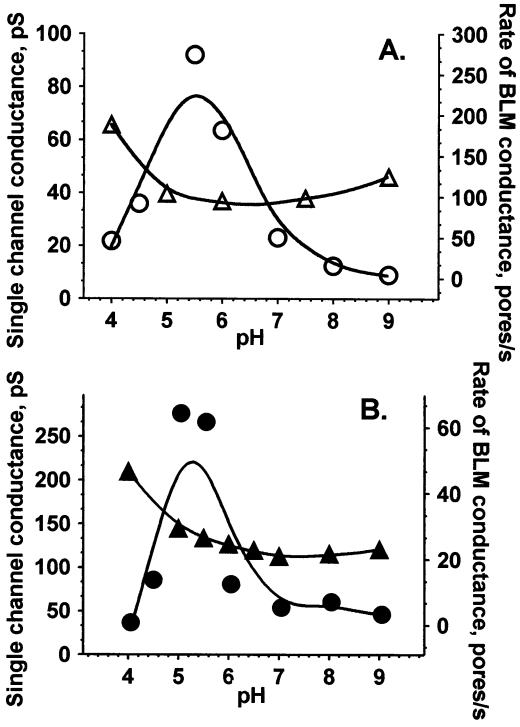

Fig. 8. pH-dependencies of the maximum rate of bilayer conductance (○, ●) and the conductance of single channel (△, ▲) induced by M-ST (*A*) and by wild ST (*B*). In experiments measuring the rate of channel formation (○) PLM was formed from phosphatidylcholine-cholesterol mixture (3:1, by mass) by the technique of Montal & Mueller. Buffer 1 was used. The toxin was added to the *cis* side of the PLM that was clamped at −20 mV. The potential was chosen to induce negligible potential-dependent channel closures. (These closures could be clearly observed at larger potentials, especially at acid pHs.) The final concentration of the toxin was kept constant and equal to 2.5 μg/ml. Two to nine experiments were carried out to obtain each value of the dependence. The mean values are represented. Other conditions are the same as in Fig. 2. The single-channel conductance experiments (△). A few hundred single-channel events were registered at each value of pH. Buffer 1 with an appropriate value of pH was used. Mean values of a single-channel conductance are represented. Final concentration of the toxin was 0.2–10 nM/ml; dependent on pH value. Other conditions are the same as in Fig. 2.

experiments for wild-ST-formed pores (*data not shown*). This value is practically equal to that obtained in the PLM-system (*see above*).

There is another method of analysis of the lysis curves which uses the values of the half-time of hemolysis to evaluate the pore size. The method assumes that the half-time value represents the time necessary for the osmoprotectant (nonelectrolyte) to diffuse inside the cell through the toxin-induced pores. Hence, the half-time value could be used to estimate the ''permeability'' of the nonelectrolyte inside the pore. A Renkin plot (Renkin, 1954; Ginsburg & Stein, 1987) reporting the relative permeability of the molecule versus its size (Fig. 7, inset), allows quantification of the functional radius of the pores. For native toxin-induced pores the radius was estimated at 1.52 ± 0.03 nm. It is slightly larger than the value established by the simple semiquantitative method (*see above*) and those published recently [Krasilnikov et al., 1988, 1991, 1992]. For M-ST-induced pores the radius was estimated at 1.66 ± 0.03 nm (Fig. 7, inset). So this *quantitative analysis of the hemolytic curves demonstrates that M-ST creates* (*in erythrocyte membranes*) *water pores with slightly larger size than native toxin does.*

Taken together, the data obtained allow the conclusion that the smaller single-channel conductance induced by M-ST (in comparison with that induced by wild ST) does not result from a decrease in the channel diameter (since the diameter is either constant or, perhaps, slightly increased). The smaller conductance might be determined by the changes in the distribution of ionogenic (titratable) groups around the channel entrances.

From all the experiments described above we can conclude that a single substitution in the glycine-rich region of ST changed most of the properties of the oligomeric ST channel. At the same time the knowledge about the properties of M-ST channels gives us a possibility to start studying the localization of Cys130 in the channel structure. It is reasonable to assume that the differences in structure of ST and M-ST molecules in solution are localized in the glycine-rich loop, the region around Cys130 in the mutated toxin. We assume that this is also true for all subunits of the channel inserted in the membrane. If these assumptions are valid the determination of Cys130 localization corresponds to the structurally altered region responsible for the observed changes in channel properties and vice versa.

M-ST-induced Ion Channels and Specific SH-Reagent

Since the results of Ward et al. (1994) point out that Cys130 is probably situated close to the second leaflet of the liposomal membrane (that corresponds to the *trans*-mouth of the channel in our PLM-system) we decided to probe its localization using SH-specific reagents: NMM, DTNB and IAA. The influence of these reagents on zero current potential and CVR parameters of M-ST premodified PLM was tested. The protocol of the experiments included two steps: (i) application of the reagent on both sides of the PLM, (ii) addition of the reagent asymmetrically—on the *cis* or on *trans* side only. Unfortunately, we were not able to detect a change in the bilayer selectivity even with the first protocol, even though the chemicals were applied for a long time (120–180 min). The characteristics of the CVR were modified by the reagents, but the changes are not significant (Table 3). It is known that the SH-group of Cys130 is easy accessible to the used reagents when M-ST is in water soluble

form (Palmer et al., 1993*b*). Hence, it is possible to conclude that the modification of the unique SH-group is not followed by changes of the tested features of the channel. Another possibility (with a much larger probability) is that this group is not available to the reagents in the structure of M-ST formed channel. (Latter assumption was strongly supported by results (Valeva et al., 1996) reported during the revision of the manuscript. Authors had shown that the residues at hinge zone of the toxin are alternately exposed to a polar and nonpolar environmental and Cys130 belongs to the latter group.) In any case *the use of the reagents did not give us an opportunity to make a decision regarding the localization of Cys130 in the ion channel structure.*

Thus we were obliged to use the indirect way of determining Cys130 localization in the channel structure—through a localization of the changes in channel structure comparing the properties of M-ST and ST channels under widely different conditions. The great possibilities of PLM-system were used to this aim.

The study of localization of the changes (that provided the established differences between ST and M-ST channels) in the channel structure.

The M-ST-induced Channel in Uncharged PLM. Clearing Up the Contribution of Positive and Negative Charges Generated by Ionogenic (Titratable) Groups in Determining Cation-Anion Selectivity of the M-ST Channel

To measure the cation/anion selectivity of a channel one usually uses different concentrations of electrolyte at *cis*- and at *trans*- sides of PLM. Investigators usually assume that the value of cation-anion selectivity is independent of the direction of the salt-gradient used. However, this dependence actually exists and can help us to clarify some features of the compared channels. One needs to be reminded that in the presence of different concentrations of an electrolyte in two compartment of the experimental cell, the Debye lengths at these two sides are different too. This means that the contribution of ionogenic (titratable) groups situated at the *cis* and at the *trans* entrances of a channel in determining the channel selectivity has to depend on the direction of the electrolyte gradient through the membrane. This gives us the possibility of examining the charge distribution between ion channel mouths and the localization of a channel in the membrane plane. To accomplish this proposition, we did a comparative analysis of the pH-dependencies of the selectivity of M-ST-induced ion channel incorporated in uncharged PC-BLM. Two different directions of KCl gradients through the membrane (300 mM/100 mM KCl, *cis*/*trans*, and 100 mM/300 mM KCl, *cis*/*trans*,—first and second types of the gradient) were used. The toxin was always added to the *cis* compartment of the experimental cell. It was found (Fig. 3*A*) that at acid pHs (pH 4.0–6.0) the values of zero current potential were practically identical for both types of gradient. To explain the data it is useful to remember that side chains of some amino acid residues contain negative (Asp, $pK_a = 3.86$; Glu, $pK_a = 4.25$; Cys, $pK_a = 8.33$ and Tyr, $pK_a = 10.1$) and positive charge (His, $pK_a = 6.0$; Lys, 10.5 and Arg, $pK_a = 12.5$; Lehninger, 1972) generated by ionogenic (titratable) groups. The side chains that are in the contact with water take part in determining an equivalent charge of the protein and only a few of them, those situated close enough to the channel entrances, determine the equivalent potential at the central zone of the entrances and the channel selectivity, respectively.

It is clear that at pH range (4.0–6.0) the contribution of the ionogenic (titratable) groups that generate negative charges in the determination of the selectivity of the M-ST channel is smaller than the contribution of positive charge groups. Hence, in the M-ST channel, the latter groups (positive charges) determine the main part of equivalent potential at both entrances of the channel. Since at pH 4.0–6.0 the values of zero current potential were practically identical for both types of gradient the contribution of this type of group in the determination of equivalent potential at the *cis* entrance of the M-ST channel is approximately equal to that at the *trans* entrance.

At pH values greater than 6.0 one can observe that the channels demonstrate larger cation selectivity with the first type of gradient (300 mM/100 mM KCl, *cis*/*trans*) than with the second type. Consequently, the equivalent potential of the M-ST channel is more negative with the first type of gradient than with the second one. From these observations one can conclude that *the contribution of negatively charged groups in the equivalent potential is larger on the* trans *entrance of the M-ST channel.*

Selectivity of M-ST Channels Incorporated in PLM with Negative Charges on the Membrane Surfaces. Are the Two Entrances of the M-ST Channel Equally Distant from the Bilayer Surfaces?

It is necessary to note that the selectivity of M-ST channels (like that of wild-ST-channels) is sensitive to surface potential of the bilayer. This gives us two possibilities to check the localization of the M-ST channel in the membrane plane. The first is based on the comparative analysis of the pH-dependencies of the selectivities of azolectin PLM (Az-PLM) at two types of KCl gradient. Azolectin is a lipid mixture containing lipids with negative charge at their polar heads. For our experiments the type of lipid used was not important but the presence of negative charges at the surface was the important vari-

Table 1. Influence of the planar lipid bilayer composition on the zero current potential of M-ST induced ion channels

Lipid composition (*cis*/*trans*)	PC/PC	Az/Az	Pc/Az	Az/PC
Zero current potential (mV)	−5.59 ± 1.58	−14.05 ± 0.51	−12.82 ± 1.32	−6.43 ± 0.60

The bilayers were formed by the union of two monolayers whose lipid composition is described in the table. Zero current potential was measured in the presence of a threefold transmembrane gradient of KCl (0.3 M/0.1 M; *cis*/*trans*). Both solutions contained 5 mM citric acid and pH was adjusted to 6.5 by Tris-OH. 5–7 experiments were carried out to obtain each value represented. The toxin was added in the *cis* compartment of the experimental chamber. Other conditions of the experiment are the same as described in the text.

able. The protocol used was the same as above in the case of the uncharged PC–PLM. It was found (Fig. 3*B*) that with the first type of the gradient (*cis*/*trans* 300/100 mM KCl) the channels incorporated in Az-PLM were always more permeable for cation than the channels in PC-PLM under identical conditions. On other hand, when we used the second type of the gradient, the dependencies obtained with AZ- and PC-bilayers were the same. Consequently, only the entrance that is situated at the *trans*-side of PLM is sensitive to the negative charges of the lipid surface of the membrane. *This points out that the* trans *entrance of the M-ST channel is much closer to the bilayer surface than the* cis *one.*

The distance between the *trans* entrance of M-ST and the polar heads of the lipid is actually short. The increase of KCl concentration at the *trans* side of PLM from 100 mM (Debye length ~0.97 nm) to 300 mM (Debye length ~0.56 nm) was practically sufficient to neutralize the influence of the negative charges of the lipid polar heads. This conclusion is supported by experiments using greater concentrations of KCl. We could not see a difference (except in sign) between values of zero current potential (about 3 mV; $P_K > P_{Cl}$) at 500 mM/1500 mM or 1500 mM/500 mM (*cis*/*trans*) gradients, at pH 7.5.

Asymmetrical Bilayers

To confirm our previous conclusion about the asymmetrical localization of the M-ST channel in the membrane plane we used asymmetrical bilayers, where one monolayer was made from PC and the other from azolectin. The toxin was applied to the *cis* side of the PLM and then the value of zero current potential was measured. The results of this set of experiments are presented in Table 1.

It was found that the value of zero current potential depended on the lipid composition of the *trans* monolayer of the PLM. When the toxin was added to a PC monolayer of a PC/Az PLM the value of zero current potential was close to that for a pure azolectin (*cis*/*trans*) PLM. On other hand when the toxin was added to an azolectin monolayer of Az/PC PLM the value of zero current potential was close to that for a pure PC (*cis*/*trans*) PLM. This implies that the entrances of the channel are at different distances from the polar heads of the membrane lipids. If we call the channel entrance which protrudes from the plane of the membrane into the side of the toxin addition the ''*cis*'' entrance and the entrance on the other side the ''*trans*'' entrance, then we can conclude that the ''*cis*'' *entrance of the channel, indeed, is placed farther from the surface of the polar lipid heads than the* ''trans'' *entrance.*

Current-Voltage Relationship and the Localization of the Structural Differences of the Wild and Mutated Channels

The analysis of CVR of M-ST and ST channels gives us another possibility to clarify the localization of differences in structures of these channels. It was shown that the CVR of wild-ST channels can be transformed to a sharply asymmetrical and nonlinear relation (that looks like the one determined in the present paper for the M-ST channel), as long as we use bilayers that have a negative potential at the *trans* surface of the PLM only (Fig. 4, insert). This observation confirms the important role of the negative charges generated by ionogenic (titratable) groups (mentioned above in the analysis of the channel selectivity) in determining M-ST-channel properties. In addition it also shows that these changes have to be mainly localized at the *trans* entrance of the channel. Application of the electrostatic approach (developed to describe the behavior of the wild ST-channel, in Krasilnikov & Sabirov, 1989; Krasilnikov et al., 1991; *for detail see Appendix 2*) to the M-ST channel supports this assumption. This theoretical description shows that the addition of about 11 negative charges to the *trans* entrance of wild ST channel is sufficient to adequately describe the properties of the M-ST channel.

The Localization of the pH-Sensitive Mouth of the Channel

The analysis of the pH dependence of CVR nonlinearity gives us another chance to clarify the structural features

Table 2. Parameters of current-voltage characteristics of the modified BLM under symmetrical and asymmetrical pH

Parameters of CVR	Values of pH*, *cis/trans*			
	8.0/8.0	5.0/5.0	8.0/5.0	5.0/8.0
Mutant-ST				
A	4.40 ± 0.34	2.06 ± 0.24	1.92 ± 0.11	5.34 ± 0.37
L_-	1.93 ± 0.08	1.33 ± 0.15	1.32 ± 0.05	2.21 ± 0.18
L_+	0.62 ± 0.04	0.74 ± 0.03	0.84 ± 0.12	0.58 ± 0.03
Wild ST				
A	1.97 ± 0.17	0.97 ± 0.09	0.63 ± 0.07	2.33 ± 0.14
L_-	1.36 ± 0.05	1.08 ± 0.08	0.81 ± 0.06	1.5 ± 0.08
L_+	0.77 ± 0.05	1.07 ± 0.02	1.19 ± 0.04	0.77 ± 0.05

Buffer 2, with pH adjusted to the appropriate value by 1M KOH and 1M citric acid, was used in these experiments. PLM was formed from an phosphatidylcholine-cholesterol mixture (3:1; by mass). The toxin was added to the *cis* compartment of the experimental chamber. * The pH value at the beginning of the experiment. The final value (that was verified at the end of experiment) could be distinguished at ±0.1 pH. Results of 3–8 experiments are represented.

of the channels. As evidenced in Fig. 5 the value of L_+ was practically constant within a pH range of 4.0–9.0. Whereas the value of L_- was strongly pH-dependent. Moreover, the established differences in CVR between the ST- and M-ST channels are also determined, mainly, by the difference in values of L_-.

The experimental data that allowed the localization of the ''pH-sensitive mouth'' of the channel formed by M-ST and by wild ST were obtained in experiments with pH shifts in one side of the bilayers. It was found that a decrease in pH-value at the *cis* side (where the toxin was added) of the PLM did not decrease the asymmetry nor the nonlinearity of CVR (Table 2). Moreover both parameters were slightly increased. However, the analogous pH shift at the *trans* side of the bilayer transformed the CVR shape deeply. It became practically equal to that obtained by the pH-shift at both sides of the PLM simultaneously (Table 2). We have found that almost all parameters of the CVR (for M-ST) obtained at pH 5.0/5.0 and 8.0/5.0 were reliably distinguished from those obtained at pH 8.0/8.0 and 5.0/8.0 ($P < 0.001$). The analogous result was obtained for PLM modified by wild toxin, but in this case the differences were not so large ($P \approx 0.05$). The differences between CVR parameters obtained at 5.0/5.0 and 8.0/5.0 or between those obtained at 8.0/8.0 and 5.0/8.0 were observed only for a few features (A and L_- for M-ST and A for wild ST) and were not large ($P \approx 0.05$). Hence, *the* trans *entrance of M-ST and wild ST channels are much more pH-sensitive than the* cis *one. The difference in the* trans *entrances of these channels is mainly responsible for the observed differences in their CVRs.*

To verify this assumption we have done a theoretical analysis with an approach recently developed for the channel formed by the wild ST (Krasilnikov & Sabirov, 1989; Krasilnikov et al., 1991, *see* Appendix 2). The results point out that the asymmetrical pH influences on selectivity and CVR could only be observed if the apparent charge of one of the mouths (the one situated far from the surface of the membrane; in the *cis* entrance) indeed depends weakly on pH. While the apparent charge of the *trans* mouth, that is closer to the surface of the second leaflet of the bilayer, has to depend strongly on pH. The comparison of the results obtained for the two channels (wild and mutant ST) demonstrates that the values of apparent charges at their trans entrances is different, and at pH 7.0 this discrepancy is maximal with values of 1.05 and −9.62 for wild and mutant ST, respectively. Consequently, *the contribution of the negative charges generated by ionogenic* (*titratable*) *groups at the* trans *entrance is much larger in the case of the M-ST channel.*

As we noted above it is most likely that the difference in structures of ST and M-ST molecules are located around Cys130 in monomers and in all membrane subunits of the channels. Then, the determination of the localization of the changes observed in the channel structure should be equivalent to the determination of Cys130 localization. If this assumption holds, since the main differences between ST- and M-ST channels were found to be at the trans entrance of the channels, we have to conclude that the Cys130 glycine-rich region of the toxin takes part in formation of the *trans* entrance of the oligomeric channel.

Another data set concerning this aspect is presented in Table 4. One can see that different treatments on ST molecules (such as protease treatments and point mutation) can bring somewhat analogous changes in the channel properties. A close analysis demonstrates that all treatments have one common feature: They all affect the central glycine-rich loop of ST. To take into account the experimental observations that the main differences between channel induced by wild toxin and the channels induced by those ''modified'' toxin molecules were shown to be located in the *trans* entrance of the channel *the data presented in Table 4 strongly argue, even if indirectly, that the localization of glycine-rich loop of ST* (*and Cys130, respectively*) *corresponds to the* trans *entrance of the oligomeric channel*. Consequently, this part of the toxin penetrates the hydrophobic zone of the bilayer and takes part in the formation of the ion channel mouth close to the second leaflet of the membrane.

As it was established the main difference in *trans* entrances is in larger value of negative charges in cases of M-ST, F-ST and K-ST channels as compared to the ST-channel.

For M-ST channel we can assume that the SH-group of Cys130 can, in principle, take part in determination of the stronger cation channel selectivity at alkaline pH

Table 3. Influence of SH-reagents on cation-anionic selectivity and parameters of current-voltage characteristics of M-ST modified BLM

Parameters	Control	NMM	DTNB	IAA
Application on BLM				
Concentration (mg/ml)		1.0	0.06	1.0
Time (min)		120	180	120
Selectivity (mV)	2.6 ± 0.5	2.9 ± 0.7	2.3 ± 0.6	2.2 ± 0.9
A	5.5 ± 0.9	5.6 ± 1.8	5.4 ± 0.3	4.9 ± 0.2#
L_-	2.16 ± 0.18	2.08 ± 0.22	1.97 ± 0.12	2.05 ± 0.21
L_+	0.56 ± 0.03	0.61 ± 0.02	0.56 ± 0.02	0.56 ± 0.05

Buffer 2 at pH 7.0 was used in these experiments. PLM was formed from an azolectin-cholesterol mixture (3:1; by mass). Zero current potential was measured in the presence of a threefold transmembrane gradient KCl (0.1 M/0.3 M; *cis/trans*). The toxin was added to the *cis* compartment. # $P * 0.05$. Other conditions of the experiment are the same as described in Materials and Methods.

Table 4. Comparative analysis of the properties of the ion channels induced by ST, its mutant and its proteolysed forms

Sample	Lytic activity	Selectivity	Asym. CVR	Place of changes
Wild ST	~1800	−12	~1.6	—
M-ST	~2000	+5	~4.5	130
F-ST#	~2.0	+6	~4.5	7–8; 130–131
K-ST	~800	+12	~4.0	133–134; 139–140; 140–141

Lytic activity is represented as HU/mg protein. PLM was formed from PC. Protein was always added to the *cis* compartment of the experimental cell. Selectivity is represented as the value of the zero current potential, mV. It was measured at 100/300 *cis/trans* KCl-system, pH 7.5. The positive sign indicates cationic selectivity of the channels. Asymmetry of CVR was measured at 100 mM KCl solution, pH 7.5. F-ST is a nicked ST (or its N-terminal fragment) obtained after weak trypsin digestion. K-ST is a nicked ST obtained after weak digestion of wild toxin with Proteinase K. # The full comparison among features of the channels formed by ST, M-ST and F-ST are presented in Figs. 3–6. Places of the changes—are the positions of the substitution in primary structure of ST molecule (M-ST) or the positions of the peptide bonds that are cleaved by the used enzymes (taken from Blomqvist et al., 1987; Thelestam & Blomqvist, 1988).

only because of its pK_a. This group is well modified by specific reagents at pH 7.5–8.0 (when M-ST is in water soluble form; Palmer et al., 1993*a*,*b*) and, consequently, its pK_a obviously is not different from most tiols' pKs (8.0–10; Hollecker, 1989). However, more likely (because SH-group of this Cys is not available to specific reagent in the channel structure) the introduction of Cys at position 130 of the primary structure of ST can simply change the structure of the glycine-rich region in such a way as to make the side chain of one or both of the two neighboring Asp-residues (127 or 128) come much closer to the channel *trans* entrance than in wild ST channels.

For the F-ST channel trypsin digestion results in cleavage of the polypeptide chain between Gly130 and Lys131 and, consequently, in the appearance of new carboxyl- and amino-groups in the glycine-rich region of the molecule. We can speculate that, because this region is flexible (after cleavage), these two new ionogenic (titratable) groups can move apart from each other in the structure of the F-ST channel. So that the alpha-carboxyl group of Gly130 is located (or remains) close to the *trans* entrance of F-ST channel, while the other group (Lys131) is situated far from that channel entrance and does not take a large part in determining the equivalent potential at the channel entrances.

Protease K can cleave the glycine-rich loop of ST in at least three positions. As a result, the toxin molecule loses six amino acid residues in the central glycine-rich region. We reason, in an analogy with the argument used for F-ST channels, that in K-ST channels an alpha-carboxyl group of Gly133 plays an important role in determining the channel properties. Larger value of cation-anion selectivity of K-ST channel in comparison with F-ST channel can be a result of larger distance of alpha-amino group of Val140 from the *trans* entrance of K-ST channel than that for Lys131 in F-ST channel.

So all of above mentioned indirect (experimental and theoretical) data suggest that the hinge part of the toxin (where Cys130 is situated) builds the ''pH-dependent *trans* mouth'' of the ion channels formed by the M-ST and, consequently, this part of the toxin penetrates the lipid bilayer. The conclusion is also in good agreement with recently published data (Ward et al., 1994) in which the authors used N-(7-nitrobenz-2-oxa-13-diazol-4-yl)-1,2-bis(hexadecanoyl)-sn-glycero-3-phosphoethanolamine as an energy acceptor. They found that the distance between acrylodan (an energy donor, that labeled Cys130) and the inner leaflet of liposome was 0.5 ± 0.02 nm.

Some other interesting data about membrane effects of M-ST and wild ST are presented in Appendix 1.

Conclusion

As can be seen, this first comparative study of wild and mutant channels in planar lipid bilayers (presented in this work) demonstrates considerable change in almost all channel features (conductance, selectivity and current-voltage relationship) induced by the mutation. Taken together, the data obtained allow the conclusion that the smaller single channel conductance induced by M-ST (in comparison with that induced by wild ST) does not result from a decrease in the channel diameter (since the diameter is either constant or, perhaps, slightly increased). The smaller conductance might be determined by the changes in the distribution of ionogenic (titratable) groups around the channel entrances.

If we call the channel entrance which protrudes from the plane of the membrane into the side of the toxin addition the ''*cis*'' entrance and the entrance on the other side the ''*trans*'' entrance, the data indicate that the main changes are at the *trans* entrance of the channel. This entrance was found to be much more pH-sensitive and situated much closer to the bilayer surface than the *cis* one. It was discovered that the contribution of the negative charges generated by ionogenic (titratable) groups at the *trans* entrance is much larger in the case of the M-ST channel.

It is reasonable to assume that the differences in structure of ST and M-ST molecules in solution are localized in the glycine-rich loop, the region around Cys130 in the mutated toxin. We assume that this is also true for all subunits of the oligomer channel inserted in the membrane. So in both cases, the local structural change around Cys130 is suggested. To take these assumptions in mind, the localization of the structurally altered region responsible for the observed changes in channel properties corresponds to localization of Cys130 in the channel structure. Hence, Cys130 is localized close to the *trans* entrance of the channel, because at this entrance the main changes were found.

Additional support for this assumption was obtained from the comparative analysis of the channels formed by wild, mutant and by protease-nicked toxins. A close analysis demonstrates that all treatments (such as protease treatments and point mutation) have one common feature: they all affect the central glycine-rich loop of ST. At the same time, all these treatments on ST molecules bring somewhat analogous changes in the channel properties. The decrease in single-channel conductance, the inversion in selectivity and the increase in the asymmetry of current-voltage relationship was observed. Moreover, in all cases the main changes was established at *trans* entrance of the channels. The theoretical analysis (*see* Appendix 2) supports the finding and demonstrates that the main difference among compared channels is in larger value of negative charges in the only *trans* entrance in cases of M-ST, F-ST and K-ST channels as compared to the ST-channel. All the data obtained strongly argues that the glycine-rich loop of ST (and Cys130, respectively) corresponds to the *trans* entrance of the oligomeric channel. The loop penetrates the hydrophobic zone of the bilayer and takes part in the formation of the ion channel mouth close to the second leaflet of the membrane.

SH-group of Cys130 was shown to be not available to the SH-reagents in the structure of M-ST formed channel and, therefore could be exposed to a nonpolar environment. Therefore, the introduction of Cys at position 130 of the primary structure of ST obviously changes the structure of the glycine-rich region in such a way as to make the side chain some of the neighboring amino acid residues, like Asp-residues (127 or 128), for example, come much closer to the channel *trans* entrance than in wild ST channel.

During the study, we successfully found that the pH-dependence of the ionic selectivity obtained in the presence of differently oriented gradients of a permeable electrolyte, the asymmetrical bilayers and asymmetrical pH shift can be helpful in a study of any type of channel incorporated in planar lipid bilayers. One can use these techniques to estimate the charge distribution between the two entrances of an ion channel and the localization of a change in the channel structure and the channel itself on the membrane plane.

We are grateful to Prof. S. Bhakdi and Dr. M. Palmer (Institute of Medical Microbiology, University of Mainz, Germany) for providing us with the protein samples and Prof. Dr. A.C. Campos de Carvalho (Institute of Biophysics, UFRJ, Rio de Janeiro, Brazil) for useful comments. We thank Dr. P. Merzlyak for his help with some BLM data collection. This work was supported by the Conselho National de Desenvolvimento Cientifico e Tecnologico (CNPq) Brasil and by Fundação de Amparo á Ciência e Tecnologia, Governo do Estado de Pernambuco (FACEPE).

References

Adair, G.S. 1929. The thermodynamic analysis of the observed osmotic pressures of protein salt in solutions of finite concentrations. *Proc. Roy. Soc. London, Series A.* **126:**16–24

Antonov, V.G. 1982. Lipids and Ion Permeability of Membranes. p. 148, Nauka, Moscow

Bard, J. 1979. Nonlinear Estimation of Parameters. Statistics. Moscow

Bergelson, L.D., Dyatlovitskaya, E.V., Molotkovsky, J.G., Batrakov, S.G., Barsukov, L.I., Prokazova, N.V. 1981. Preparative Biochemistry of Lipids. p. 105, 155, Nauka, Moscow

Bhakdi, S., Muhly, M., Fussle, R. 1984. Correlation between toxin binding and hemolytic activity in membrane damage by staphylococcal α-toxin. *Infect. Immun.* **46:**318–323

Bhakdi, S., Tranum-Jensen, J. 1988. Damage of cell membranes by pore-forming bacterial cytolysins. *Prog. Allergy* **40:**1–43

Bhakdi, S., Tranum-Jensen, J. 1991. S. aureus alpha-toxin. *Microbiol. Rev.* **55:**733–751

Bhakdi, S., Weller, U., Walev, I., Martin, E., Jonas, D., Palmer, M. 1993. A guide to use of pore-forming toxins for controlled perme-

abilization of cell membranes. *Med. Microbiol. Immunol.* **182:**167–175

Blomqvist, L., Bergman, T., Thelestam, M., Jörnvall, H. 1987. Characterization of domain borders and of a naturally occurring major fragment of staphylococcal α-toxin. *FEBS Lett.* **211:**127–132

Blomqvist, L., Thelestam, M. 1986. A staphylococcal alpha-toxin fragment: Its characterization and use for mapping biologically active regions of alpha-toxin. *Acta Path. Microbiol. Immunol. Scand. Sect. B.* **94:**277–283

Eler, H. 1972. Statistical method for approaching. AINP Report, P11-6816, p. 27, Dubna

Forti, S., Menestrina, G. 1989. Staphylococcal alpha-toxin increases the permeability of lipid vesicles by cholesterol and pH-dependent assembly of oligomeric channels. *Eur. J. Biochem.* **181:**767–773

Fussle, R., Bhakdi, S., Sziegoleit, A., Tranum-Jensen, J., Kranz, T., Wellensiek, H.L. 1981. On the mechanism of membrane damage by S. aureus α-toxin. *J. Cell Biol.* **91:**83–94

Ginsburg, H., Stein, W.D. 1987. Biophysical analysis of novel transport pathways indiced in red blood cell membranes. *J. Membrane Biol.* **96:**1–10

Gray, G.S., Kehoe, M. 1984. Primary sequence of the alpha-toxin gene from *Staphylococcus aureus* Wood 46. *Infect. Immun.* **46:**615–618

Hebert, H., Olofsson, A., Thelestam, M., Skriver, E. 1992. Oligomer formation of staphylococcal alpha-toxin analyzed by electron microscopy and image processing. *FEMS Microbiol. Immunol.* **105:**5–12

Hollecker, M. 1989. Counting integral numbers of residues by chemical modification. *In:* Protein Structure. A Practical Approach. T.E. Creighton, editor. p. 147, Information Press LTD, Oxford

Ikigai, H., Nakae, T. 1985. Conformational alteration in alpha-toxin from S. aureus concomitant with the transformation of the water-soluble monomer to the membrane oligomer. *Biochim. Biophys. Acta* **30:**175–181

Jonas, J.C., Li, G., Palmer, M., Weller, U., Wollheim, C.B. 1994*a*. Dynamics of Ca^{2+} and guanosine 5′-[gamma-thio]triphosphate action on insulin secretion from alpha-toxin-permeabilized HIT-T15 cells. *Biochem. J.* **301:**523–529

Jonas, D., Walev, I., Berger, T., Liebetrau, M., Palmer, M., Bhakdi, S. 1994*b*. Novel path to apoptosis: small transmembrane pores created by Staphylococcal α-toxin in T-lymphocytes evoke internucleosomal DNA degradation. *Infect. Immun.* **62:**1304–1312

Kagawa, Y., Racker, E. 1971. Partial resolution of the enzymes catalyzing oxidative phosphorilation. *J. Biol.Chem.* **246:**5477–5487

Kato, I., Watanabe, M. 1980. Chemical studies on staphylococcal alpha-toxin and its fragments. *Toxicon* **18:**361–365

Katsu, T., Ninomiya, C., Kuroko, M., Kobayashi, H., Hiroto, T., Fujita, Y. 1988. Action mechanism of amphypathic peptides gramicidin S and melittin on erythrocyte membrane. *Biochim. Biophys. Acta* **939:**57–63

Krasilnikov, O.V., Muratkhodjaev, J.N., Zitzer, A.O. 1992. The mode of action of *Vibrio cholerae* cytolysin. The influence on both erythrocytes and planar lipid bilayers. *Biochim. Biophys. Acta* **1111:** 7–16

Krasilnikov, O.V., Sabirov, R.Z. 1989. Ion transport through channels formed in lipid bilayers by S. aureus α-toxin. *Gen. Physiol. Biophys.* **8:**213–222

Krasilnikov, O.V., Sabirov, R.Z., Ternovsky, V.I. 1991. Proteins, ionic channels and regulation of ion transport through membranes. B.A. Tashmukhamedov, editor. pp. 3–208, FAN, Tashkent

Krasilnikov, O.V., Sabirov, R.Z., Ternovsky, V.I., Merzliak, P.G., Muratkhodjaev, J.N. 1992. A simple method for the determination of the pore radius of ion channels in planar lipid bilayer membranes. *FEMS Microbiol. Immunol.* **105:**93–100

Krasilnikov, O.V., Sabirov, R.Z., Ternovsky, V.I., Merzliak, P.G., Tashmukhamedov, B.A. 1988. The structure of S. aureus α-toxin induced ionic channel. *Gen. Physiol. Biophys.* **7:**467–473

Krasilnikov, O.V., Sabirov, R.Z., Ternovsky, V.I., Tashmukhamedov, B.A. 1986. Kinetic of increase of lipid bilayer conductance induced by staphylotoxin. *Biol. Membrane* **3:**1049–1056

Krasilnikov, O.V., Ternovsky, V.I., Merzliak, P.G., Zachidova, L.T., Hungerer, K.-D. 1993. Effects of monoclonal antibodies on α-staphylotoxin action against erythrocytes and model phospholipid membranes. *Biochim. Biophys. Acta* **1182:**94–100

Krasilnikov, O.V., Ternovsky, V.I., Tashmukhamedov, B.A. 1981. Properties of ion channels induced by α-staphylotoxin in bilayer lipid membranes. *Biofisica* **26:**271–275

Laemmli, U.K. 1970. Cleavage of structural proteins during the assembly of the head of the bacteriophage T_4. *Nature* **227:**660–685

Lehninger, A.L., 1972. Proteins: the amino acid building blocks: *In:* Biochemistry. The Molecular Basis of Cell Structure and Function. pp. 67–88. Worth Publishers, New York

Markin, V.S., Chizmadjcu, Yu. A. 1974. Induced Ion Transport. Yu. A. Ovchinnikov, editor. pp. 1–251. Nauka, Moscow

Menestrina, G. 1986. Ionic channel formed by S. aureus α-toxin: voltage-dependent inhibition by divalent and trivalent cations. *J. Membrane Biol.* **90:**177–190

Menestrina, G., Belmonte, G., Parisi, V., Morante, S. 1992. Structural features of the pore formed by Staphylococcus aureus alpha-toxin inferred from chemical modification and primary structure analysis. *FEMS Microbiol. Immunol.* **105:**19–28

Montal, M., Mueller, P. 1972. Formation of bimolecular membranes from lipid monolayers and a study of their electrical properties. *Proc. Natl. Acad. Sci. USA* **69:**3561–3566

Mueller, P., Rudin, D.O., Tien, H.T., Wescott, W.C. 1963. Methods for the formation on single bimolecular lipid membranes in aqueous solution. *J. Phys. Chem.* **67:**534–535

Olofsson, A., Kaveus, U., Hacksell, I., Thelestam, M., Hebert, H. 1990. Crystalline layers and three-dimensional structure of Staphylococcus aureus alpha-toxin. *Mol. Biol.* **214:**299–306

Olofsson, A., Kaveus, U., Thelestam, M., Hebert, H. 1992. The three-dimensional structure of trypsin-treated Staphylococcus aureus alpha-toxin. *J. Struct. Biol.* **108:**238–244

Palmer, M., Jursch, R., Weller, U., Valeva, A., Hilgert, K., Kehoe, M., Bhakdi, S. 1993*a*. S aureus alpha-toxin. Production of functionally intact, modifiable protein by introduction of cysteine residues. *Med. Microbiol. Immunol.* **182:**207

Palmer, M., Jursch, R., Weller, U., Valeva, A., Hilgert, K., Kehoe, M., Bhakdi, S., 1993*b*. Staphylococcus aureus alpha-toxin. Production of functionally intact, site-specifically modifiable protein by introduction of cysteine in positions 69, 130, 186. *J. Biol. Chem.* **268:**11959–11962

Palmer, M., Weller, U., Messner, M., Bhakdi, S. 1993*c*. Altered pore-forming properties of proteolytically nicked staphylococcal alpha-toxin. *J. Biol. Chem.* **268:**11963–11967

Renkin, E.M. 1954. Filtration, diffusion and molecular sieving through porous cellulose membranes. *J. Gen. Physiol.* **38:**225–243

Sabirov, R.Z., Krasilnikov, O.V., Ternovsky, V.I., Merzliak, P.G. 1993. Relation between ionic channel conductance and conductivity of media containing different nonelectrolytes. A novel method of pore size determination. *Gen. Physiol. Biophys.* **12:**95–111

Sabirov, R.Z., Zakhidova, L.T., Krasilnikov, O.V. 1991. Three types of pores formed by S. aureus α-toxin in erythrocyte membranes. *Biol. Membrany* **8:**749–754

Six, H., Harshman, S. 1973. Physical and chemical studies on staphylococcal alpha-toxin A and B. *Biochemistry* **12:**2677–2683

Thelestam, M., Blomqvist, L. 1988. Staphylococcal alpha-toxin—Recent advances. *Toxicon* **26:**51–65

Ternovsky, V.I., Zaripova, R.K., Krasilnikov, O.V., Korneev, A.S.,

1991. Comparative analyze of properties of ion channels induced by staphylococcal alpha-toxin and it's N-terminal fragment. *Biol. Membrany* **8:**271–279

Tobkes, N., Wallace, B.A., Bayley, H. 1985. Secondary structure and assembly mechanism of an oligomeric channel protein. *Biochemistry* **24:**1915–1920

Valeva, A., Walev, I., Pinkernell, M., Bayley, H., Palmer, M., Bhakdi, S. 1996. Molecular architecture of toxin channel delineated by fluorometric analyses of cysteine-substituted mutants: resistant cells prevent membrane insertion of pore-forming domain. *Medical Microbiology and Immunology* **185:**119

Walker, B., Bayley, H. 1994. A pore-forming protein with a protease-activated trigger. *Protein Eng.* **7:**91–97

Walker, B., Krishnasastry, M., Bayley, H. 1993. Functional complementation of staphylococcal α-hemolysin fragments. Overlaps, nicks, and gaps in the glycine-rich loop. *J. Biol. Chem.* **268:**5285–5292

Walker, B., Krishnasastry, M., Zorn, L., Bayley, H. 1992. Assembly of the oligomeric membrane pore formed by Staphylococcal alpha-hemolysin examined by truncation mutagenesis. *J. Biol. Chem.* **267:**21782–21786

Walker, B., Krishnasastry, M., Zorn, L., Kasianowicz, J., Bayley, H. 1992. Functional expression of the α-hemolysin of S. aureus in intact E. coli and in cell lysates. Deletion of five C-terminal amino acids selectively impairs hemolytic activity. *J. Biol. Chem.* **267:**10902–10909

Ward, R.J., Leonard, K. 1992. The Staphylococcus aureus alpha-toxin channel complex and the effect of Ca^{2+} ions on its interaction with lipid bilayers. *J. Struct. Biol.* **109:**129–141

Ward, R.J., Palmer, M., Leonard, K., Bhakdi, S. 1994. Identification of a putative membrane-inserted segment in the α-toxin of Staphylococcus aureus. *Biochemistry* **33:**7477–7484

Watanabe, M., Kato, I. 1978. Purification and some properties of a lethal toxic fragment of staphylococcal alpha-toxin by tryptic digestion. *Biochim. Biophys. Acta* **535:**388–400

Appendix 1

pH Dependencies of the Rate of the Channel Formation

To study the pH dependence of the M-ST channel formation we observed an interesting effect: the maximum pore formation rate happened at pH 5.5–6.0 (Fig. 8*A*). The same pH effects were observed using wild ST and other channel-forming toxins (Krasilnikov et al., 1986; Krasilnikov, Muratkhodjaev & Zitzer, 1992). In all cases pH changed the ion channel distribution between closed and open states. A possible physico-chemical explanation of the phenomenon was developed recently (Krasilnikov et al., 1986, 1989, 1991). It is based on two experimental facts: (i) a process of transition of the preformed nonconducting oligomer (pre-channel) to open the conductive state (channel) is the limiting rate of pore formation; (2) the similarity in the bell-shaped pH-dependencies of rate of channel formation and the Gibbs free energy of interaction of ionogenic (titratable) groups of such channel-forming protein-toxins with water. As was shown by Krasilnikov et al. (1986, 1989, 1991) about 10 ionogenic amino acid residues (titratable charges) are sufficient to describe the shape and localization of the maximum point on the pH-dependence of channel-forming activity for wild-type ST. This maximum was also at the same pH range (Fig. 8*B*) where it was observed for M-ST. Hence, the same quantitative and qualitative composition of ionogenic groups (titratable charges) of the toxin can determine the opening phenomenon in the case of M-ST.

The presence of the pH-optimum for channel-formation and localization of the optimum (5.5–6.0) on the pH scale would favor the use of this toxin as a chemotherapeutical antitumour medicine. This hypothesis should be tested in vivo, but now it is supported by the fact that the pH value of the extracellular medium bathing the tumor cells could be 0.4–1.0 pH-unit lower than that of the intestinal fluid of normal tissues.

Appendix 2

The electrostatic approach to describe properties of ST-channel was developed as described elsewhere (Krasilnikov & Sabirov, 1989). In short, the ion transport through ST channels was described assuming ion diffusion and migration in an asymmetrically charged water pore and considering the interactions of penetrating ions with fixed charges at the channel entrances. For an arbitrary profile of potential energy in a membrane and equilibrium at the channel entrances the partial current density was determined according to Markin & Chizmadzhev (1974) by:

$$I_i = Z_i\lambda_I RT/F[C_i^1\exp(Z_i\psi) - C_i^2] / \int_0^\delta \{\exp[Z_i\psi(1 - X/\delta) + W_i]\}dx \quad \text{(A1)}$$

where Z_i is the charge of ion *i;* λ_I is the equivalent electrical conductance; δ is the channel length; X is the channel length coordinate which is zero at the *trans* entrance of the channel and δ at the *cis* one; W_i is the potential energy of the ion in the pore, in kT; $\Psi = \Psi_o + \varphi_1 - \varphi_2$ is the intermembrane potential, in kT/e; C_i^1 and C_i^2 are equilibrium ion activities at the *cis*- and *trans* entrances, connected with ion activity in water solution, C_o, by the Boltzman relationship:

$$C_i = C_o \exp(-Z_i\varphi_i) \quad \text{(A2)}$$

where

$$\varphi_i = eQ_i \exp(-r/L_D) \quad \text{(A3)}$$

is the equivalent potential generated by the titratable charges at the channel entrances; Q_i is the total charge at the respective entrance; r is the channel radius; L_D is Debye length equal to

$$L_D = 1/(F\sqrt{(\epsilon\,\epsilon_o\,RT/2C_o)}) \quad \text{(A4)}$$

e, π, ϵ, ϵ_o, T, R, F and k have their usual meaning.

Considering the interactions of ions with charges at the channel entrances, the potential energy profile may be expressed as

$$W_i = Z_i\,\varphi_1 \exp[(X - \delta)/L_D] + Z_i\,\varphi_2 \exp(-X/L_D) + E \quad \text{(A5)}$$

E has to be included due to several reasons. First, ions in the channel

are subject to an action of image forces (Markin & Chizmadzhev, 1974). Moreover, hindrance to the ion movement due to friction forces should also be considered (Antonov, 1982). The principal peculiarity of the latter forces is their independence on the charge sign of the penetrating ions. For simplicity X-independent E was taken for the first approximation. The total current is the product of the sum of partial currents and the channel cross section square. It was calculated as

$$I = \pi r^2 \Sigma I_i. \quad \text{(A6)}$$

For comparing arbitrary channels the values of 1.3 nm and 10 nm were taken for the radius and length, respectively. Q_1, Q_2 and E were unknown parameters. To obtain these we used the experimental values of CVR and zero current potentials. Parametrization was carried out by the least square method using minimum random search algorithm (Eler, 1972). The computations were performed on IBM PC AT. Confidence intervals for the parameters were found using the Monte-Carlo method (Bard, 1979). The integral in equation (A5) was obtained numerically by the trapezium formula.